Hindawi
International Journal of Antennas and Propagation
Volume 2017, Article ID 4563571, 7 pages
https://doi.org/10.1155/2017/4563571

Research Article

Reconfigurable Antenna for Jamming Mitigation of Legacy GPS Receivers

İsmail Şişman[1] and Korkut Yeğin[2]

[1]*Department of Electrical and Electronics Engineering, Yeditepe University, 34755 Istanbul, Turkey*
[2]*Department of Electrical and Electronics Engineering, Ege University, 35100 Izmir, Turkey*

Correspondence should be addressed to Korkut Yeğin; yegink@gmail.com

Received 11 October 2016; Revised 26 February 2017; Accepted 23 March 2017; Published 30 April 2017

Academic Editor: Ikmo Park

We propose a simple solution for jamming mitigation of L1 band GPS by electronically switching antenna beam for wide and narrow beamwidths. Assuming the jamming signal is directed from low elevation angles, antenna reception can be made significantly lower at these angles by electronically reconfiguring the antenna beamwidth. Four-element antenna array and one of the elements of the array are designated as antijam (array) mode and normal mode of the antenna. The antenna is placed on a degenerate-ground with symmetric slots in the ground. Front-end configuration for this antenna is also discussed. Simulations and measurements are performed to validate the proposed design. The antenna achieves more than 15 dB rejection in measurements and more than 20 dB cross-polarization improvement compared to standalone (normal mode) antenna. The system can easily be replaced with existing active antenna to improve antijam capability of the receiver.

1. Introduction

Positioning and localization systems using satellite systems are increasing rapidly with the introduction of new services. Currently there are four satellite positioning systems (GPS, GLONASS, GALİLEO, and BEIDOU) which offer growing number of applications ranging from automotive to medical systems [1, 2]. Such widespread use of satellite navigation also causes attention on system vulnerability to intentional and unintentional attacks. In particular, considerable research has been devoted to malicious attacks such as jamming and spoofing. These attacks may deny service or even deceive or divert the navigation functionality [3].

To overcome and counteract such attacks, many potential solutions have been proposed in the past. To counteract possible threats, high performance systems with phased array antennas have been offered [4–8]. These systems identify the location of the threat and place a null on that direction and a maximum of the pattern along the satellite direction. These are particularly important for missile and unmanned aerial vehicle navigation and they are usually coupled with inertial navigation systems and dead-reckoning algorithms. In civil applications, automatic landing of an aerial vehicle or unmanned control of a ground vehicle also requires such precise positioning and localization.

On the software side, lessons learned from multipath mitigation have been largely transformed and developed substantially for mitigation of spoofing. Deception or spoofing of GNSS receivers is usually a threat for military applications in a hostile environment. Software defined GNSS receivers are usually well suited to cope with spoofing threats. Most of these countermeasures require substantial changes either on the hardware or on the software/firmware or both [9–11].

For instance, a phased array approach which enables the receiver to locate the direction of jammer and place a null in that direction requires completely a new antenna and a receiver. Likewise, to counteract spoofing, a new software or firmware must be installed in the receiver. Unfortunately, most of these remedies require significant changes in the receiver hardware or the firmware. These approaches are useful for military applications, but they are vastly expensive for many civil applications. A low-cost solution on the

hardware without the need for a software or firmware update and without the need for a change in the receiver is definitely needed. Hence, a low-cost solution must involve only the active antenna and should not replace the receiver and be complaint with existing legacy receivers such as the amount of DC current that can be drawn and supplied to the low noise amplifier of the antenna. One solution to this problem is presented in this study.

First of all, most civil applications of GNSS are terrestrial excluding the commercial applications for aerial vehicles. In addition, GPS is the most common service provider among others. Hence, in our study, we target civil GPS applications for vehicles on the ground [12–14]. Jamming signals for these receivers are mostly terrestrial as well and originate from low elevation angles contrary to high elevation satellite signals. This assumption naturally provides some immunity to terrestrial jammers, but since the GPS signal is below thermal noise floor, its jamming signal does not need to be powerful which makes them relatively simple and easy to operate. The motivation of this study is to provide enhanced immunity to terrestrial jammers with only changing the antenna unit but keeping legacy receiver unchanged including its firmware. We provide a simple and affordable solution that increases the immunity to jamming more than 10 dB compared to standalone antenna-receiver unit. The antenna front-end is basically switched ON and OFF for wide and narrow beamwidths depending on the presence of a jammer. In the next section, we discuss the antenna unit. Then, we provide front-end configuration that is to be used in place of legacy existing low noise amplifier (LNA) unit. Numerical and experimental data for the pattern reconfigurable beamwidths are presented in Section 4.

2. Design of the Antenna

Most vehicle mounted GPS units use a ceramic patch antenna with 25 × 25 × 4 mm in size with substrate relative permittivity around 20 as illustrated in Figure 1. This antenna, when mounted on vehicle's metallic roof or trunk, provides about 3.5 to 4 dBic gain at zenith with 1.8 dB axial ratio and becomes linear vertically polarized at low elevation angles. We placed four of these ceramic patches in an array configuration and assigned one of the array elements as the main or normal antenna. The antenna structure is shown in Figure 2. Sequential rotation of array elements by 90° and proper phasing for each antenna element ensured right-hand circular polarization (RHCP) gain in array mode. With low-insertion loss switches in the feed network, we were able to switch from default mode main antenna to array antenna (antijam mode) or vice versa. The switches are controlled by the RF front-end where a power detector continuously samples the signal and when the sampled signal exceeds the threshold the switches are turned on for array mode. Otherwise, the default mode of operation is single antenna operating alone as the main antenna.

First, antenna element separation for array and single antenna modes was optimized for performance. The main criteria in this optimization were array antenna gain, single antenna gain, low elevation rejection of array antenna, and antenna input impedance match for both modes of operation. To improve array and single mode antenna gains, slots in the antenna ground plane were placed to create degenerated ground structure. The slots were symmetrical with respect to antenna placement. With degenerated ground structure,

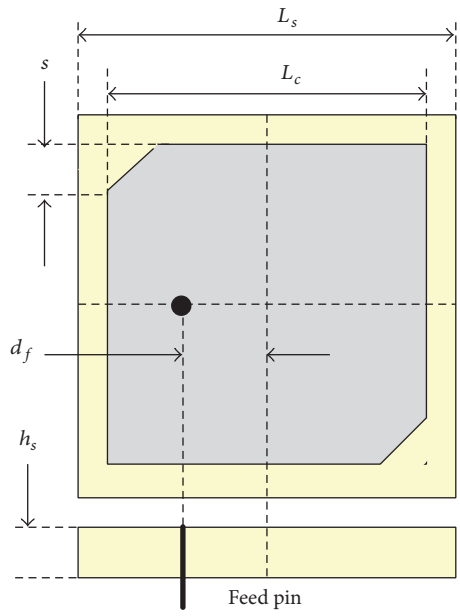

Figure 1: Commercial ceramic patch antenna configuration. L_s = 25 mm, L_c = 20 mm, s = 1.75 mm, d_f = 9.5 mm, and h_s = 4 mm.

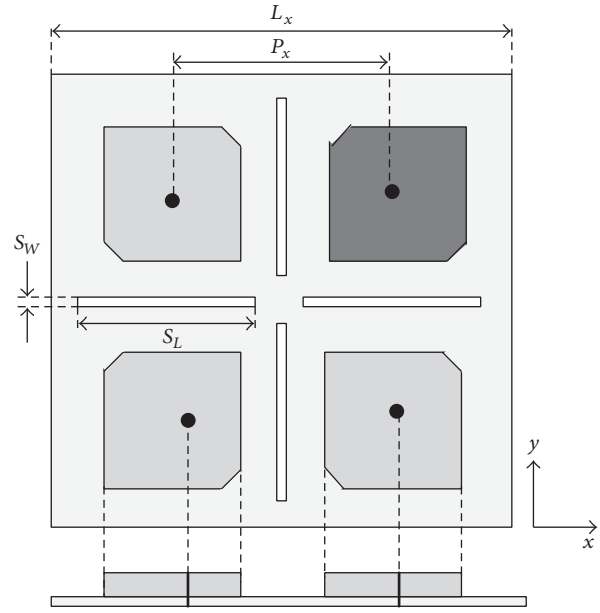

Figure 2: Four-element antenna configuration. In normal mode only upper-right antenna is used. In antijam mode, all four antennas are utilized. L_x = 190 mm, P_x = 92 mm, S_L = 82 mm, and S_W = 2 mm.

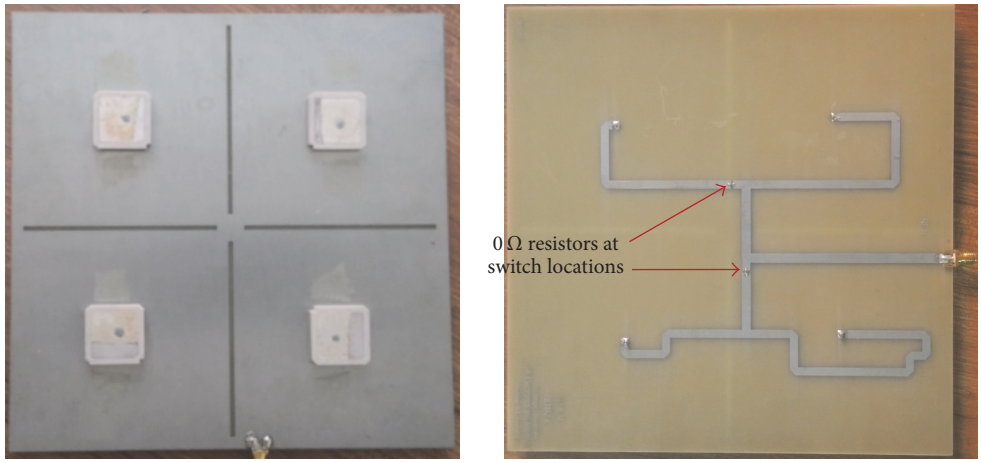

(a) (b)

Figure 3: Realized antenna: (a) top side, ceramic patches; (b) bottom side, feed network.

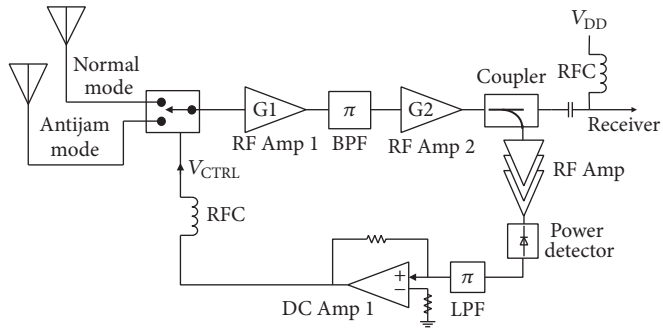

Figure 4: Front-end of the antenna.

single antenna (normal mode) and array antenna (anti-jam mode) performance satisfied our target expectations. Antenna simulation and measurement results are presented in Section 4.

Array antenna elements were placed with $0.48\lambda_o$ separation. This choice of element spacing was arrived through numerical optimization of the full antenna structure. It also provided excellent rejection at low elevation angles as discussed in Section 4.

Prototype antenna and the feed network are displayed in Figure 3. The feed network was realized on Rogers 4003 substrate ($\varepsilon_r = 3.38$, $\tan\delta = 0.0027$). Zero-ohm resistors were soldered in places of switches for ease of antenna pattern measurements. DC bias lines were omitted in this prototype, but they could be easily integrated to the feed structure with no degradation on RF performance.

3. Front-End Configuration

Front-end structure with switch control circuitry is shown in Figure 4. Low noise amplifier of the antenna consists of two amplifiers with a band pass filter in between [12]. At the output of the LNA, 10 dB coupler is placed and coupled port is fed to 3-stage RF gain amplifier to increase the signal power for power detector threshold limit. The output of the detector produces DC voltage and this voltage is first filtered out through a low-pass filter and then amplified for switch control voltage. The produced voltage can be fed to both switches simultaneously. Loop bandwidth is set by LPF and attack time for the jamming signal is mainly determined by the power detector. The power detector is a zero-bias Schottky device which requires minimal power consumption on the circuitry. Most receivers can supply DC current in the range of 60–80 mA to the LNA and total DC consumption of the proposed configuration complies with this current requirement. 5 LNAs consume less than 45 mA of DC current; hence, total current drawn from the receiver is within the limits of safe DC operation.

For antenna switch, Skyworks AS169-73LF GaAs switch with 0.3 dB insertion loss is chosen. Simulated parameters of the front-end are summarized in Table 1.

4. Simulation and Measurement Results

The feed network was simulated in NI Microwave Office for phase and amplitude at antenna ports as shown in Figures 5 and 6. It was observed that power variation was less than

Table 1: Simulated antenna front-end parameters.

Parameter	Value
Gain	32 dB
Input P1 dB	−24 dBm
Output IP3	+18 dBm
Noise figure	1.3 dB
I/O reflection coefficient (1575.4 MHz +/− 10 MHz)	<−10 dB
Dynamic range (assuming strong L1 signal at −110 dBm level)	>86 dB

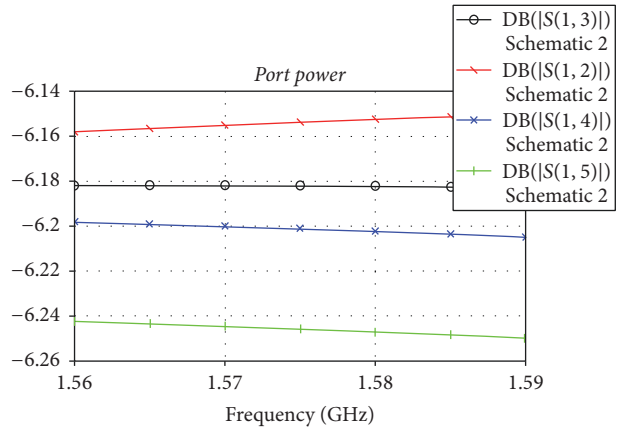

Figure 5: Feed network port-power simulation in Microwave Office. Port 1 indicates the common port, and ports 2 through 5 represent patch antenna feed pins.

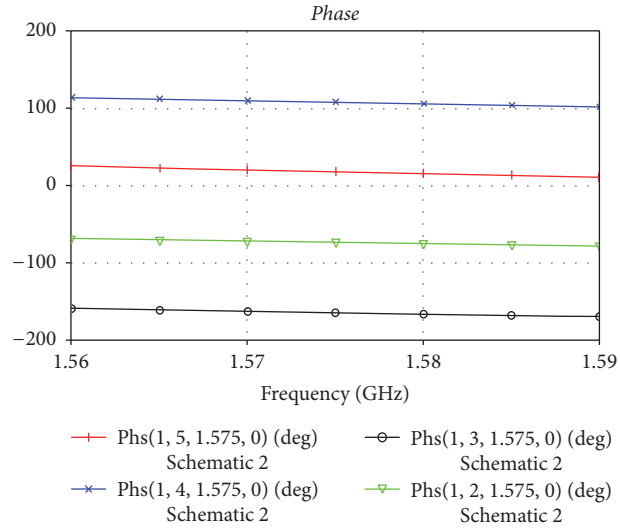

Figure 6: Feed network port-phase simulation in Microwave Office. Port 1 indicates the common port, and ports 2 through 5 represent patch antenna feed pins.

0.25 dB and phase deviation from 90° phase progression was less than 8°.

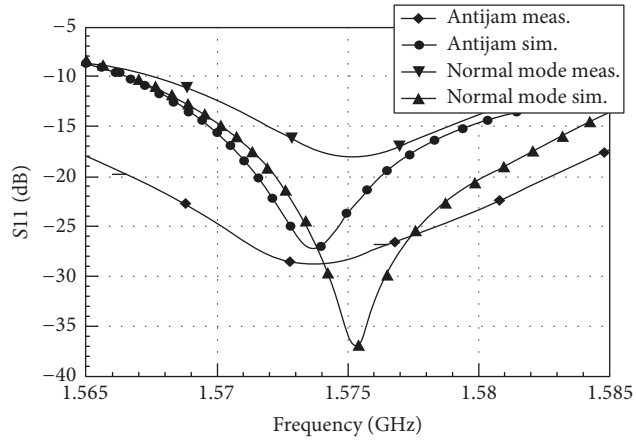

Figure 7: Input impedance match of designed antenna for normal and antijam modes.

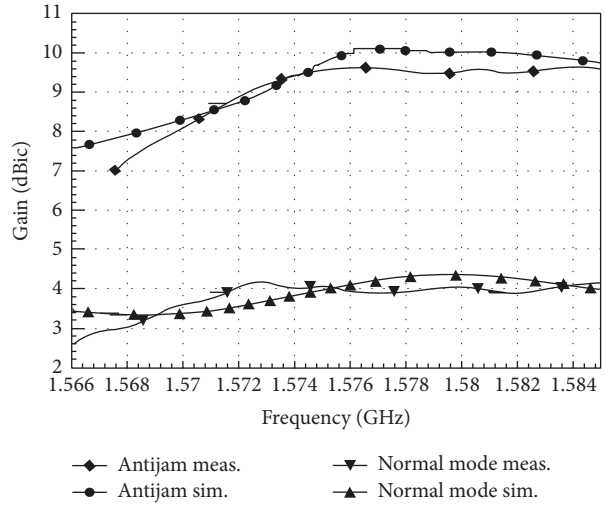

Figure 8: RHCP gain of antenna for normal and antijam modes.

Simulated and measured antenna input impedance match for normal and antijam modes are displayed in Figure 7. The input impedance match for +/− 10 MHz relative to center frequency (1575.4 MHz) is quite good and no worse than the impedance match of the ceramic patch itself.

RHCP gain of the antenna for both modes of operation as a function of frequency is shown in Figure 8. At design frequency, antijam mode achieved 9.5 dBic gain whereas normal mode had 4 dBic gain. Measurements mostly corroborated with simulations with at most 0.5 dB deviation across the measured bandwidth. Typical axial ratios of the commercial ceramic patches are less than 2 dB across 20 MHz bandwidth. We observed the similar characteristics with standalone and array antenna as phase and amplitude match in simulations were quite satisfactory. Measured axial ratio of the array antenna was no greater than 1.93 dB.

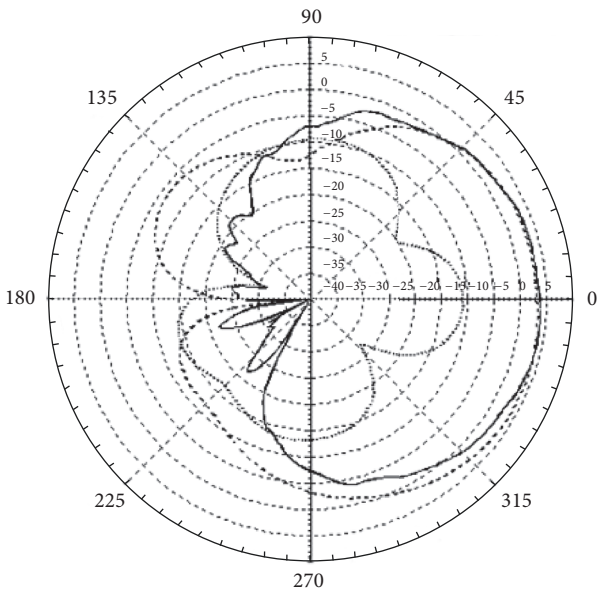

Figure 9: Normal mode radiation patterns ($\phi = 0$ cut, elevation plane).

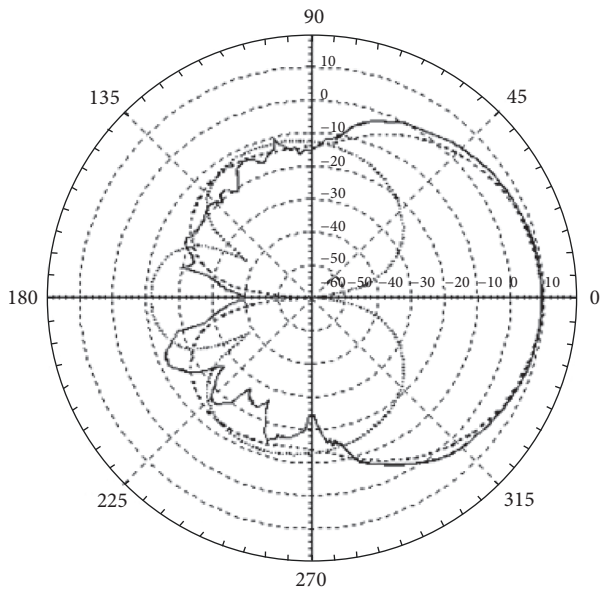

Figure 10: Antijam mode radiation patterns ($\phi = 0$ cut, elevation plane).

Elevation radiation patterns at $\phi = 0$ for normal and antijam modes are given in Figures 9 and 10, respectively. Especially at low elevation angles, our measured data deviated from simulated ones due to our measurement setup. Although we performed measurements in anechoic chamber, back scattering from the antenna-rotator was believed to be responsible for deviations at low elevation angles.

Zenith cuts ($\theta = 0$) RHCP and LHCP for both modes are presented in Figures 11 and 12, respectively. Antijam mode (array mode) cross-polarization levels were significantly lower than normal mode ones, which was highly desirable for mitigation of multipath effects.

We also simulated low elevation angle normal and antijam modes as a function of frequency as shown in Figure 13. In particular, antijam (array) mode exhibited significant improvement (more than 20 dB) over normal mode (standalone) antenna in simulations.

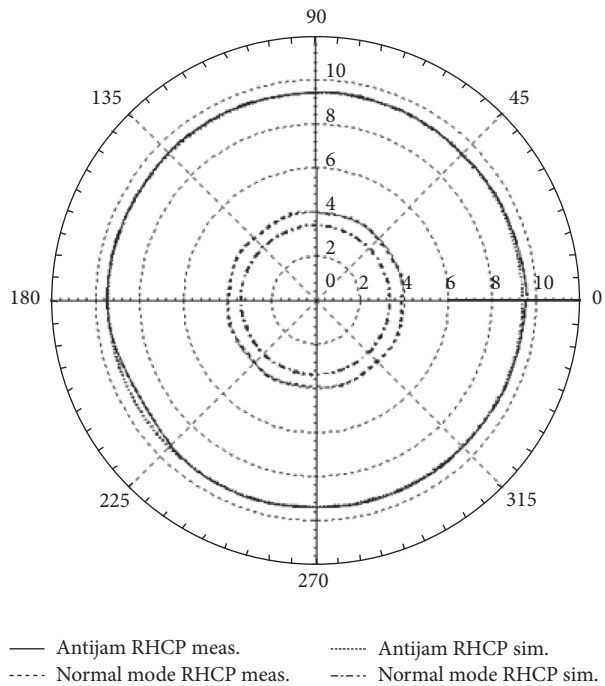

Figure 11: Zenith cut azimuth plane for antijam and normal modes for RHCP.

5. Conclusions

Reconfigurable pattern antenna was proposed and realized for jamming mitigation of GPS L1 band where most commercial applications exist. Proposed solution is directly applicable to existing legacy GPS receivers without any change on the hardware or the firmware. It only replaces the antenna-LNA combination. Existing ceramic patch antennas were used which were low-cost and easy to obtain. Antenna ground plane structure and feed lines were optimized for phase coherency and performance. In simulations, resistance to low elevation jamming signals was 20 dB better than standalone antenna, and in measurements we observed about 16 dB improvement, which was mainly due to our imperfect measurement setup. Our antenna provides a simple and cost-effective solution to intentional or unintentional jamming of L1 band GPS signals.

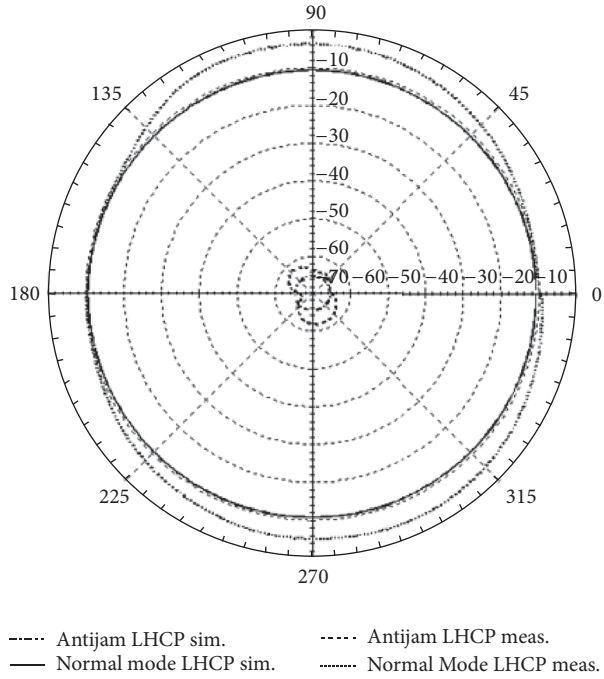

Figure 12: Zenith cut azimuth plane for antijam and normal modes for LHCP.

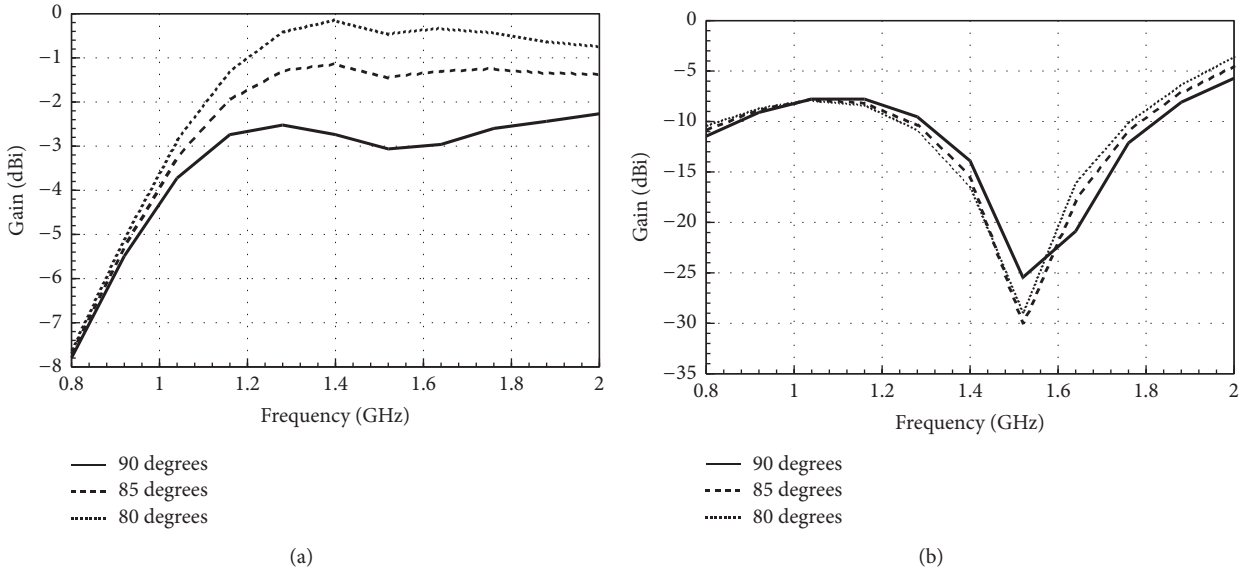

Figure 13: Near-terrestrial (θ = 90, 85, 80) linear vertical gain, (a) normal mode, and (b) antijam mode.

Conflicts of Interest

The authors declare that they have no conflicts of interest.

Acknowledgments

This work is partly supported by Ministry of Science, Industry, and Technology of Turkey under SANTEZ Grant no. 0786.STZ.2014 and Ege University, EBILTEM, under Grant no. 2015/BİL/008.

References

[1] E. D. Kaplan and C. J. Hegarty, *Understanding GPS: Principles and Applications*, Artech House, Norwood, Mass, USA, 2006.

[2] G. Liu, L. Xu, and Y. Wang, "Modified dual-band stacked circularly polarized microstrip antenna," *International Journal of Antennas and Propagation*, vol. 2013, Article ID 382958, 5 pages, 2013.

[3] B. M. Ledvina, W. J. Bencze, B. Galusha, and I. Miller, "An in-line anti-spoofing device for legacy civil GPS receivers," in

Proceedings of the International Technical Meeting (ITM '10), pp. 868–882, San Diego, Calif, USA, January 2010.

[4] M. Trinkle and W.-C. Cheuk, "Null-steering GPS dual-polarised antenna arrays," in *Proceedings of the 6th International Symposium on Satellite Navigation Technology Including Mobile Positioning & Location Services (SatNav '03)*, Melbourne, Australia, July 2003.

[5] R. Di, H. Qin, and X. Li, "Research of GPS anti-jamming based on circular antenna array," *Data Science Journal*, vol. 6, pp. S782–S788, 2007.

[6] D. S. De Lorenzo, *Navigation accuracy and interference rejection for GPS adaptive antenna arrays [Ph.D. thesis]*, Stanford University, 2007.

[7] S. Rougerie, G. Carrié, F. Vincent, L. Ries, and M. Monnerat, "A new multipath mitigation method for GNSS receivers based on an antenna array," *International Journal of Navigation and Observation*, vol. 2012, Article ID 804732, 11 pages, 2012.

[8] S. Caizzone, G. Buchner, and W. Elmarissi, "Miniaturized dielectric resonator antenna array for GNSS applications," *International Journal of Antennas and Propagation*, vol. 2016, Article ID 2564087, 10 pages, 2016.

[9] Y. D. Zhang and M. G. Amin, "Anti-jamming GPS receiver with reduced phase distortions," *IEEE Signal Processing Letters*, vol. 19, no. 10, pp. 635–638, 2012.

[10] L. Li, B. Li, H. Chen, and F. Wang, "Phase errors simulation analysis for GNSS antenna in multipath environment," *International Journal of Antennas and Propagation*, vol. 2015, Article ID 962627, 8 pages, 2015.

[11] D. Pepe, L. Vallozzi, H. Rogier, and D. Zito, "Design variations on planar differential antenna with potential for multiple, wide, and narrow band coverage," *International Journal of Antennas and Propagation*, vol. 2015, Article ID 478453, 13 pages, 2015.

[12] K. Yegin, "AMPS/PCS/GPS active antenna for emergency call systems," *IEEE Antennas and Wireless Propagation Letters*, vol. 6, pp. 255–258, 2007.

[13] K. Yegin, "On-vehicle GPS antenna measurements," *IEEE Antennas and Wireless Propagation Letters*, vol. 6, pp. 488–491, 2007.

[14] K. Yegin, "Instrument panel mount GPS antenna," *Microwave and Optical Technology Letters*, vol. 49, no. 8, pp. 1979–1981, 2007.